

# Morphology and Charge Transport in Conjugated Polymers

R. J. KLINE AND M. D. McGEHEE

Department of Material Science & Engineering, Stanford University,  
Stanford, CA, USA

*Determining the relationship between charge transport and morphology is key to increasing the charge carrier mobility of conjugated polymers. This review details a fundamental study of the charge transport and morphology of regioregular poly(3-hexylthiophene) and sets out general principles for obtaining high charge carrier mobilities. The basis for this study was the finding that despite being more crystalline, low molecular weight films have a substantially lower mobility than high-MW films. An examination of this apparent contradiction is used to provide insight into how the charge carriers move through a conjugated polymer film and provide a model for charge transport.*

**Keywords** thin-film transistor, polymer morphology, polythiophene, charge transport, grazing incidence x-ray diffraction, and conjugated polymer

## 1. Introduction

Conjugated polymers are being investigated for use in low-cost, large-area applications such as light-emitting diodes (LEDs),<sup>[1,2]</sup> photovoltaics (PV),<sup>[3,4]</sup> and thin-film transistors (TFTs).<sup>[5–8]</sup> Charge transport in conjugated polymers is important to the performance of both PVs<sup>[9,10]</sup> and TFTs. In TFTs, the drive current, threshold voltage, and operating frequency are the key parameters.<sup>[7]</sup> The drive current and operating frequency are determined by device geometry and the charge carrier mobility. Moore's law clearly shows the effect of reducing the channel length on the operating frequency in silicon transistors. Reducing the channel length also increases the drive current. In polymer TFTs, reducing the channel length is not always an option due to the limited resolution of the commonly used low-cost fabrication methods. Additionally, Chabinye et al. have shown that polymer TFTs with dimensions less than 10  $\mu\text{m}$  no longer obey the gradual channel approximation.<sup>[11]</sup> The overall device area of TFTs used to drive display pixels is limited to a fraction of the pixel size, so increasing the channel width to increase drive current is not an option. Finally, the capacitance of the dielectric could be increased by reducing the insulator thickness or increasing the dielectric constant. Both of these options can only provide limited increase in current since they both tend to increase manufacturing costs. Since device geometry alone is not sufficient to increase

Received 25 July 2005; Accepted 26 September 2005.

Address correspondence to M. D. McGehee, Department of Material Science & Engineering, Stanford University, Stanford, CA 94305, USA. E-mail: mmcgehee@stanford.edu

TFT performance, the charge carrier mobility of the semiconductor is thus the key parameter for improving TFT performance.

### 1.1 Charge Transport in Conjugated Polymers

The charge transport of conjugated polymers has been studied for nearly two decades. Early work focused on developing conjugated polymers as plastic conductors and tried to increase the conductivity,  $\sigma$ , to that of the inorganic metals.<sup>[2]</sup> This was accomplished by highly doping the polymer and stretch orienting the films. Polyacetylene,<sup>[12–14]</sup> polyaniline,<sup>[15–17]</sup> and polythiophene<sup>[18–20]</sup> were the predominant polymers studied for conductor applications. In 1986, the first functional polymer TFT was reported by Tsumura et al.<sup>[21]</sup> In a TFT, a large modulation of conductivity is desired between the on-state and the off-state. Doping increases the threshold voltage and since polymer TFTs are an accumulation-mode transistor, a large reverse gate voltage would be required to turn a doped channel off. Doping is thus undesirable in TFTs and therefore conductivity is not a meaningful measurement of charge transport for TFT materials. The advent of TFTs shifted the charge transport focus from conductivity to charge carrier mobility,  $\mu$ . Conductivity is fairly straightforward to measure with either two-point or four-point measurements depending on the sample to be measured. In the simplest case the resistance between two electrodes is measured and converted into conductivity. The charge carrier mobility is slightly more complicated to measure because the carrier concentration,  $n$ , must also be determined in order to convert conductivity into mobility (Eq. (1)). Alternatively, the mobility can be determined by measuring the carrier velocity,  $v$ , at a given electric field,  $E$ .

$$\sigma = ne\mu, \quad \mu = vE \quad (1)$$

The primary methods for measuring charge carrier mobility in conjugated polymers are time-of-flight (TOF),<sup>[22–25]</sup> pulse-radiolysis time-resolved-microwave-conductivity (PR-TMRC),<sup>[26–28]</sup> modeling space-charge-limited-current diodes (SCLC),<sup>[25,29–32]</sup> and modeling TFTs. The mobilities in conjugated polymers are usually too low to be measured by the Hall effect. TOF, PR-TMRC, and SCLC measure the bulk mobility of films. TOF can determine the electric field dependence of the mobility but works best on thick films ( $>1 \mu\text{m}$ ) since the transit distance must be at least ten times longer than the absorption depth to assume that all carriers travel the same distance. Determining the TOF-mobility of films with a distribution of mobilities (dispersive transport) is also complicated since the arrival of carriers at the electrodes is spread out. Additionally the mobility measured with TOF is usually biased towards the fastest carriers in the film. PR-TMRC is a contactless measurement, so the measurement is guaranteed to be the intrinsic property of the material studied and is not affected by the presence of metal electrodes. The primary limitation of PR-TMRC is that the carriers only move a small distance in the applied microwave field and the measurement can also be dominated by the fastest carriers. SCLC allows the measurement of charge transport in thin-films similar to those used in PV cells. The primary limitation of the SCLC measurement is that both the carrier concentration and electric field continuously vary across the channel, making it difficult to measure the carrier or field dependence of transport. The other limitation is that electrons and hole mobilities cannot be measured with the same device, since the work function of one of the electrodes has to be adjusted to make the device either a hole-only or electron-only diode. Expressions for both

field-dependent and field-independent cases have been developed to extract mobility from the SCLC IV curves.

It is well-known that the mobilities measured with TFTs are several orders of magnitude higher than those measured with other techniques. It was usually assumed to be due to morphology effects since all of the transport in TFTs occurs within 5 nm of the gate dielectric and the other techniques measure the mobility normal to the substrate. Additionally, conjugated polymer films usually have the chain backbone preferentially lying in the plane of the substrate. Since the chain backbone is expected to provide good transport,<sup>[28]</sup> the in-plane transport would be expected to be better. Tanase et al. provided an alternative explanation for the difference in mobility in the two directions in amorphous films by pointing out that the charge carrier concentration is several orders of magnitude higher in TFTs than in other devices and that the mobility is charge carrier concentration dependent.<sup>[33]</sup> In films such as regioregular poly(3-hexylthiophene) (P3HT) that crystallize, the insulating side chain axis typically orients vertically, inhibiting charge transport normal to the substrate.<sup>[34]</sup> These crystalline films with preferential ordering would be expected to also have a strong morphology component to the mobility difference between TFTs and diodes in addition to the carrier concentration.<sup>[35]</sup>

The apparent carrier dependence in mobility can be explained by two different mechanisms. In disordered semiconductors with hopping between localized states, increasing the carrier concentration fills the deepest traps and reduces the average trap depth.<sup>[36]</sup> This effect is the basis of the carrier dependent mobility in the variable range hopping model of Vissenberg and Matters that has been used to describe polymer TFTs.<sup>[37]</sup> When the semiconductor becomes partially ordered semiconductors, it is no longer clear that the assumptions of variable range hopping are valid. Delocalization of the charge carriers over several molecules create extended states. Salleo et al. have used the mobility edge model to describe these films.<sup>[38]</sup> The mobility edge model is similar to the multiple trap and release model used to describe amorphous silicon and crystalline small molecule organics.<sup>[39–41]</sup> The apparent carrier dependence of the mobility of TFTs is actually due to the fact that only a small portion of the carriers induced by the gate are mobile. Most of the carriers are trapped in localized states in the band tail and screen the gate field. Increasing the gate voltage increases the fraction of carriers above the mobility edge, resulting in an increase in the number of mobile charges and thus the effective mobility.

## 1.2 Morphology in Conjugated Polymers

Since the chain length of polymer molecules is considerably less than the channel length of TFTs or the thickness of diodes, charges traveling through a film must hop between molecules to get from one electrode to the other. Hopping between molecules is related to the intermolecular overlap of neighboring molecules, which is clearly dependent on how molecules pack on each other. Additionally, conjugated molecules are typically longer than the persistence length, so a charge is not expected to be able to travel the full length of a molecule before having to hop to a neighbor. The persistence length in a solid state film is generally also related to the chain packing. Therefore the chain packing is critical to charge transport.

Initial conjugated polymers were intractable due to the lack of side chains. The addition of side chains lowers the melting temperature and increases the solubility by separating the conjugated backbones and the reducing the rigidity of the backbone. The separation of the backbones by the side chains reduces the intermolecular overlap,

and thus impedes hopping of charges between molecules. This separation of the conjugated backbones is beneficial in light-emitting diodes since intermolecular overlap promotes excimer formation. Molecules for LEDs are typically designed to form amorphous films, since the packing associated with crystalline aggregates decreases the power efficiency due to excimers. These molecules typically have asymmetric, bulky side chains that cause the molecules to twist. The twisted molecules cannot pack efficiently. Conjugated polymers that crystallize tend to be more rigid and planar. Poly(3-hexylthiophene) is a classic example. The regiorandom version has a twisted chain conformation with poor packing and low crystallinity while the regioregular version has a planar conformation with efficient packing and better intermolecular overlap.<sup>[42,43]</sup> The regioregular version has a several order of magnitude higher charge carrier mobility with the polarons delocalized over several molecules.<sup>[44–46]</sup>

Morphology of conjugated polymers has been primarily analyzed through atomic force microscopy (AFM) and x-ray diffraction (XRD).<sup>[47]</sup> AFM images the surface morphology, but does not provide direct information on the film bulk or the region near the interface with the gate dielectric, which is where all of the TFT current travels. AFM images of conjugated polymers are also very sensitive to tip effects since the molecules tend to frequently contaminate the tip during imaging.<sup>[48]</sup> XRD provides information on the spacing and orientations of crystal planes. Prosa et al. used XRD to show that regioregular P3HT had a novel side chain packing structure compared to regiorandom<sup>[49]</sup> and that higher order peaks need to be used to correctly calculate the crystal size from peak widths by including the effect of non-uniform strain.<sup>[50]</sup> XRD of thin-films generally only measures the crystal planes with lattice vectors normal to the surface and samples the entire thickness of the film. In order to look at the in-plane packing in thin-films, grazing incidence x-ray scattering (GIXS) is required. GIXS is a surface sensitive technique where the penetration depth can be controlled to the first few monolayers by adjusting the incidence angle.<sup>[51,52]</sup> GIXS has been used to show that high mobility P3HT films tend to have crystals with their  $\pi$ -stacking direction preferentially oriented in-plane.<sup>[34,48,53–58]</sup> GIXS has also been used to extensively study the morphology of many other conjugated polymers.<sup>[59–62]</sup> The main limitation of x-ray measurements is that semiconducting polymers are often semicrystalline and the x-rays primarily analyze the structure of the crystalline regions. The amorphous fraction of these films is usually large enough to affect charge transport. Near-edge x-ray absorption fine structure (NEXAFS) measures the average orientation of the molecular orbitals, thus providing information on both the crystalline and amorphous regions of the film. NEXAFS has recently been used to measure the average surface orientation of conjugated polymers.<sup>[63–65]</sup>

## 2. Dependence of Charge Carrier Mobility and Morphology on Polymer Molecular Weight

The molecular weight (MW) of a rigid rod polymer like P3HT would be expected to affect the morphology. Conjugated polymers are typically thought of as semicrystalline films with small ordered domains and large amounts of amorphous material. Molecules in low-MW polymer films should be able to crystallize into a structure more like that obtained with high-mobility small molecules like pentacene. Molecules in high-MW films would be expected to be kinetically limited from forming large crystalline domains. Conventional theory on charge transport in organic semiconductors would predict that the more ordered, low-MW films should have higher charge carrier

mobility than their less-ordered, high-MW counterparts. We have shown that in reality the opposite is true. The charge carrier mobility determined by TFTs of regioregular P3HT spin cast from chloroform on HMDS-treated substrates decreases four orders of magnitude when the MW is reduced by one order of magnitude (Fig. 1).<sup>[66]</sup> This trend of increasing mobility with MW was also observed in SCLC diodes, although it was only a factor of 15 increase from low to high.<sup>[31]</sup>

Morphology analysis of the films clearly show that the low-MW films are in fact substantially more crystalline than the high-MW films. AFM images comparing low-MW films to high-MW films show that the low-MW films have rodlike crystals whereas no features indicating crystallinity can be seen in high-MW films (Fig. 2). Since the width of the rods of low-MW films corresponds to the length of the molecules, the molecules must be oriented perpendicular to the length of the rods. X-ray diffraction shows that the low-MW films do in-fact have substantially more crystals with their alkyl chains oriented out-of-plane than the high-MW films (Fig. 3a). XRD also shows that the low-MW film has some out-of-plane  $\pi$ -stacking. In-plane diffraction from GIXS measurements curiously shows that both films primarily have in-plane alkyl stacking with very little in-plane  $\pi$ -stacking (Fig. 3b). For low-MW films, the combination of alkyl and  $\pi$ -stacking in both the in-plane diffraction and the out-of-plane diffraction suggests that a large distribution of crystal orientations exist in the film. Rocking curves confirmed the existence of crystals with different orientations. Figure 3c compares the rocking curve of a low-MW film to that of a medium-MW film. A high-MW film is not shown because the Bragg peak was so weak compared to the background that it is difficult to correctly subtract out the reflectivity component. The rocking curve of the low-MW film shows a broad distribution of crystals whereas the medium-MW film has a very narrow distribution of orientations. The key thing to note about the medium-MW film out-of-plane diffraction is that more than 95% of the Bragg peak is from these highly oriented crystals. The importance of these highly oriented crystals for charge transport will be discussed further in section 4. The broad distribution of crystals in low-MW films suggest a structure like that shown in Fig. 4a. Since the alkyl side chains are insulating, P3HT crystals can only conduct in two-dimensions. This anisotropy results in a

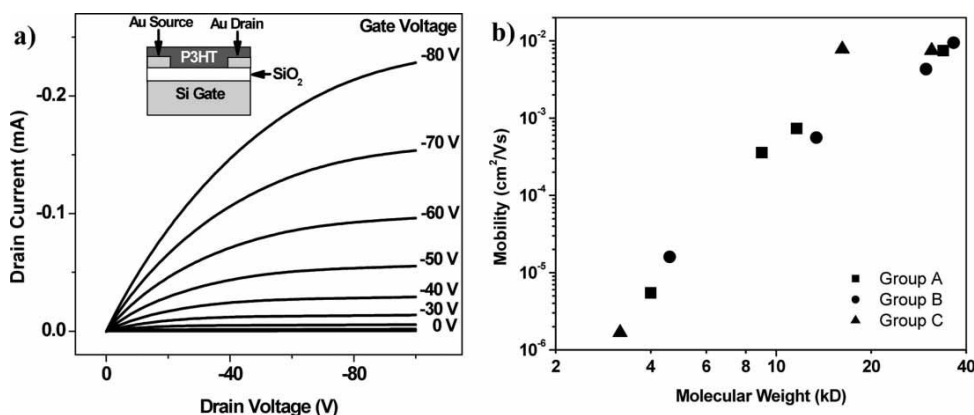


**Figure 1.** Results of transistors with varying molecular weight. a) Current-voltage curves of a 10- $\mu$ m long by 40- $\mu$ m wide transistor with a molecular weight of 33.8 kD. The inset shows a diagram of the device structure. b) Plot of field-effect mobility versus the number average molecular weight.<sup>[66]</sup>

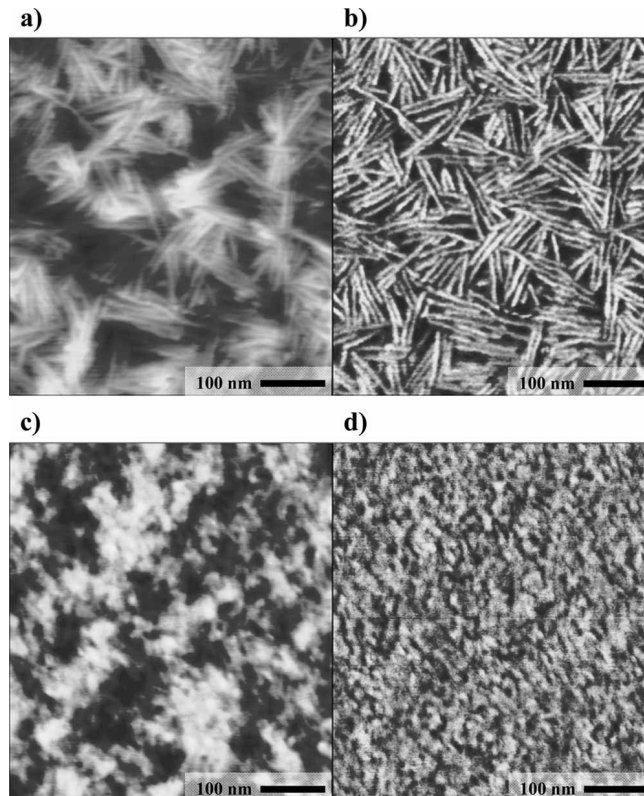


**Figure 2.** Tappingmode atomic force microscope (AFM) images. Shown are a 3.2-kD polymer film [(a) topography and (b) phase] with rms roughness = 6.6 Å and a 31.1 kD polymer film [(c) topography and (d) phase] with rms roughness = 5.8 Å.<sup>[66]</sup>

number of combinations of grain boundaries. Any grain boundary where one crystal face consists of alkyl chains will block inter-grain charge transport. Inter-grain transport can also be limited by the poor overlap between the neighboring grains. As shown by the structure of Fig. 4a and that of rodlike crystals illustrated in Fig. 5, it is clear that inter-grain transport is severely limited in the low-MW films due to the poor connectivity between grains and the large number of insulating grain boundaries. In the case of the high-MW films, there are no well-defined grain boundaries. Since the molecules are much longer than the size of the ordered domains, individual molecules are expected to be part of several domains. These bridging molecules limit the amount of misorientation between neighboring domains and provide a possible pathway for charges to go between neighboring domains.<sup>[67]</sup>

### 3. Modifying Morphology at a Constant MW

The results of the previous section suggest that the MW effect on mobility is mostly due to morphology, but they cannot rule out an inherent difference in charge transport due to chain length. Two possible explanations for improved transport with longer chains exist. The first is that charge transport along the chain is expected to be better than hopping between chains.<sup>[28]</sup> Longer chains would reduce the number of hopping events

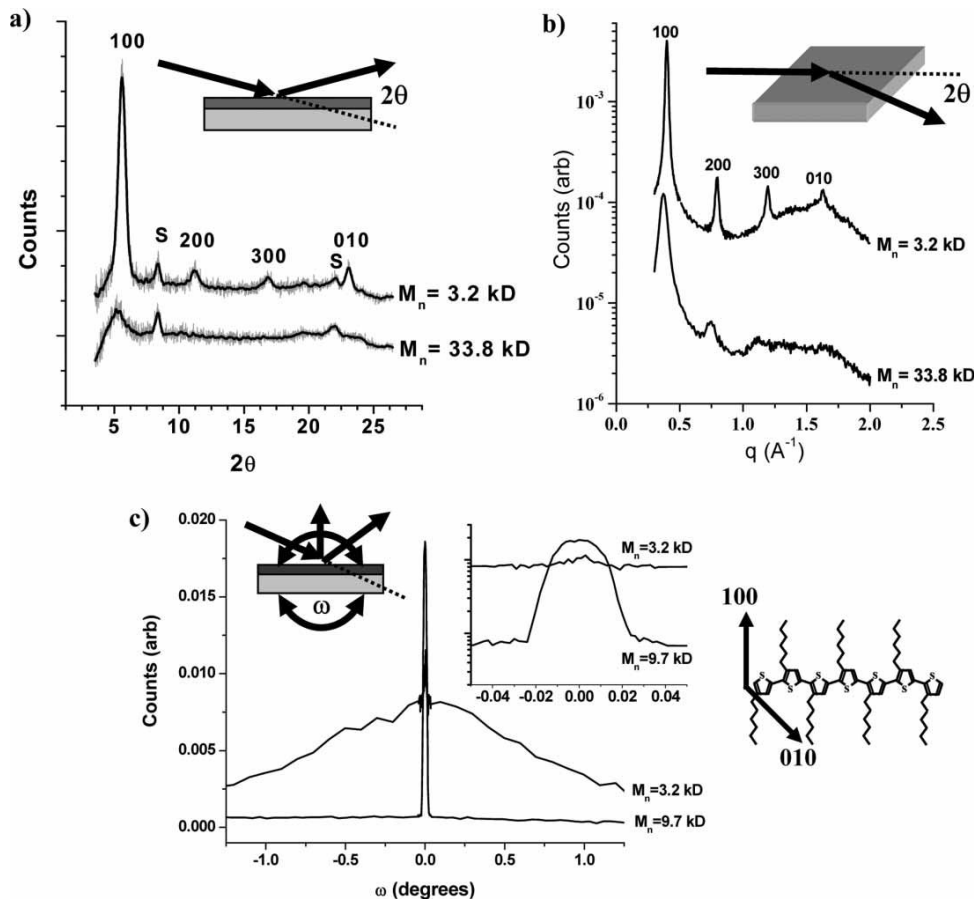


**Figure 3.** X-ray diffraction (XRD) analysis of films of various MW. a) Out-of-plane and b) in-plane diffraction of low and high-MW films cast from chloroform on HMDS treated substrates. c) Results of rocking curves on the (100) peak of a low and medium-MW film. Inset is zoomed in on log scale. The peaks labeled S are not from the polymer film; they are from either the substrate or the sample mount.<sup>[66]</sup>

and thus increase the effective mobility. The main problem with this argument is that it is unlikely that the high-MW molecules are defect free along their entire length. In reality, the high-MW molecules should be treated as a number of smaller segments of conjugation separated by insulating defects such as kinks and twists. These defects interrupt the overlap of neighboring p-orbitals and thus break the conjugation. The other explanation is that the longer chains of the high-MW films reduce the ordering threshold for bandlike transport compared to low-MW films. Beljonne et al. have used theoretical modeling to show that this is the reason that the charge transport in disordered polymers is close to that of polycrystalline small molecules.<sup>[68]</sup> In order to determine whether the mobility versus MW trend was due to morphology or chain length, the morphology was modified at a constant MW to decouple the variables of morphology and chain length. Unfortunately the difference in chain length between low and high-MW is so large that it is not possible to get the same morphology for both a low and high-MW film.

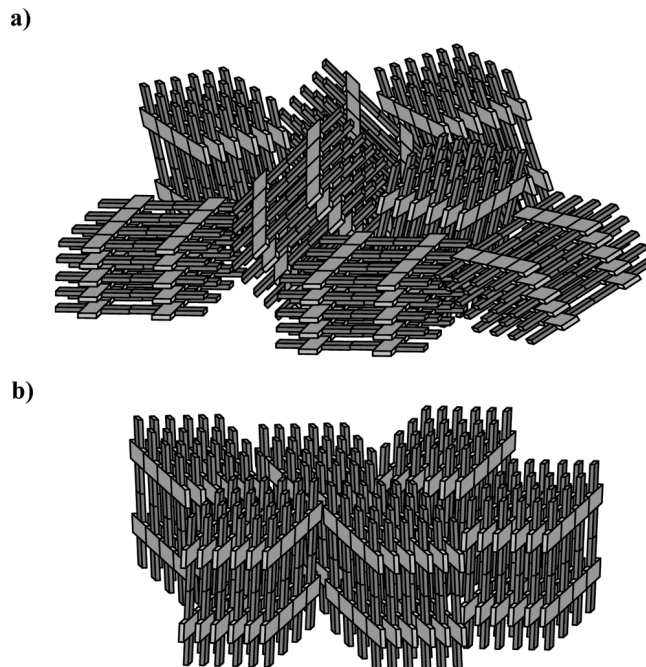


**Figure 4.** Possible packing of crystals at the buried interface. a) Case with randomly oriented grains and lots of in-plane insulating grain boundaries. b) Case with highly oriented crystal and conducting in-plane grain boundaries. Conducting  $\pi$ -stacking planes are colored with light grey and insulating hexyl chains with dark grey. Crystals are reduced in size for clarity.

Processing variations were used to modify the morphology at constant MWs. Films were annealed, spin-cast from a higher boiling point solvent, and drop-cast. Substantial variations in mobility were observed for the low-MW films while the mobility of high-MW films varied only slightly with processing conditions (Fig. 6). Each of the three processing modifications increased the mobility of the low-MW films up to one hundred times the as-spun from chloroform case. In each case, the difference between low and high-MW films was reduced to two orders of magnitude, but a trend of increasing mobility with increasing MW was still observed. The large variation in mobility of the low-MW films with processing suggests that the low-MW mobility is limited by morphology.

As expected, morphology measurements show considerable change in the low-MW films with processing conditions. AFM images clearly show a change in the packing of the rodlike crystals of the low-MW films (Fig. 7). In each case, both the length of the rods and the overlap between neighboring rods increases. The AFM images clearly suggest that charge transport between neighboring rods should be better as the rods appear to be connected better. In the case of the drop-cast film, the rods are several microns long. AFM images of high-MW films showed minimal changes with processing. XRD showed that the out-of-plane alkyl stacking peak intensity increased with processing changes for a constant MW (Fig. 8). This indicates that the number of crystals oriented with their alkyl peaks normal to the substrate has increased. Additionally the Bragg peaks are sharper, indicating that the crystals are larger. GIXS shows that the in-plane  $\pi$ -stacking increases while the in-plane alkyl-stacking decreases in cases where the mobility at a constant MW increases (Figs. 9a and b). The GIXS measurements also



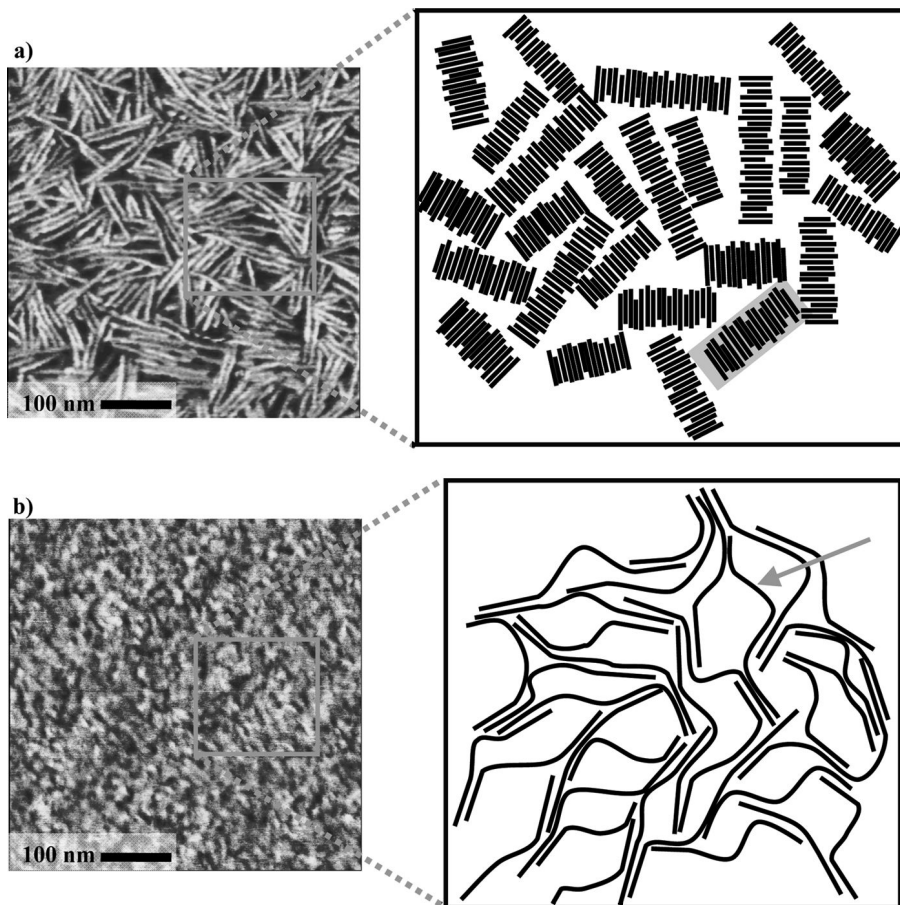


**Figure 5.** Model for transport in low and high-MW films. a) Charge carriers are trapped on nanorods (highlighted in grey) in the low MW case. b) Long chains in high-MW films bridge the ordered regions and soften the boundaries (marked with arrow).<sup>[48]</sup>

show that the peaks become sharper with processing. GIXS shows no change in the in-plane packing in cases where the mobility does not change. The correlation between in-plane  $\pi$ -stacking and mobility agree with what has been shown previously by Sirringhaus et al.<sup>[34]</sup> The key result of the GIXS measurements comes from comparing low-MW films to high-MW films with similar processing (Figs. 9c and d). These comparisons show that there is a shift in lattice spacing for the alkyl stacking with low-MW films having a smaller spacing<sup>[69]</sup> and that the low-MW films have much sharper peaks. The most important difference occurs with the in-plane  $\pi$ -stacking. In the case of the annealed films, the high-MW film has a mobility eighty times larger than the low-MW film despite having substantially less in-plane  $\pi$ -stacking. Clearly the relationship between mobility and in-plane  $\pi$ -stacking cannot explain the mobility-MW difference.

The remaining question is whether the improved mobilities of low-MW films occur because of the increased overlap of neighboring rods shown in the AFM images or due to the increased in-plane  $\pi$ -stacking. Rocking curves can provide a better understanding of what happens to the morphology of low-MW films with processing and an answer to

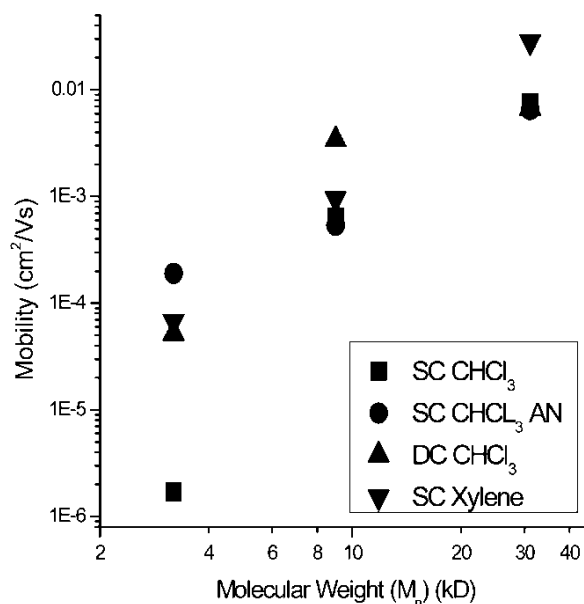


**Figure 6.** Comparison of change in charge carrier mobility for three different MWs as the processing conditions are changed. Samples are spin-cast (SC) from chloroform, annealed (AN), drop-cast (DC), or spin-cast from xylene.<sup>[48]</sup>

this question. Figure 10 shows rocking curves of the low-MW film before and after annealing. Clearly, annealing increases the number of crystals with their side-chains oriented normal to the substrate. The annealed film also has an increased concentration of highly oriented crystals compared to the as-spun film. Since the  $\pi$ -stacking direction of these crystals is perpendicular to the out-of-plane alkyl stacking, one would expect an increase of in-plane  $\pi$ -stacking with the change in crystal orientation observed with annealing as observed. Furthermore, the increased number of crystals with their side chains oriented normal to the substrate means that fewer crystals can have their side chains oriented in-plane and thus there will be fewer insulating grain boundaries in the plane of charge transport. The better connectivity observed in the AFM images is due to neighboring rods having similar orientations and thus better inter-grain transport. The increase in the in-plane  $\pi$ -stacking is simply a measure of this change in crystal orientation that results in better intra-grain transport and higher mobility.

#### 4. Modifying Surface Treatment of the Substrate at a Constant MW

In the previous sections, rocking curves showed the presence of a large population of crystals oriented within 0.03 degrees of the substrate normal (resolution of the instrument) in some of the P3HT films. These highly oriented crystals are substantially more oriented than would be expected for polymer crystals. Previous measurements of P3HT crystal orientation used a lower resolution set-up and reported distribution widths of 12–40 degrees.<sup>[56]</sup> The two possible locations to have such highly oriented crystals are the substrate and the air-film interface. Surface-induced ordering has been previously observed in liquid crystals and block copolymers at both the substrate and air interfaces, although the degree of orientation is typically less.<sup>[52,70–72]</sup> Crystals in the film bulk could

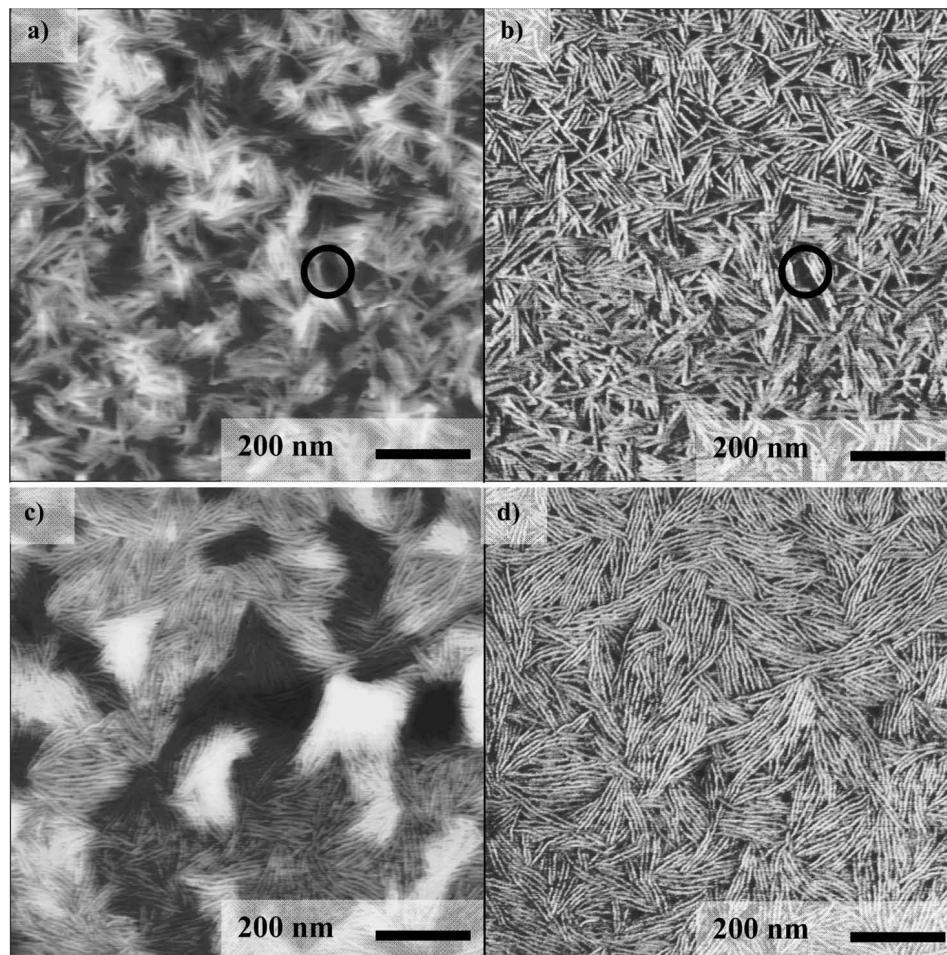


**Figure 7.** Atomic force microscope images comparing low-MW films. Samples are spin-cast from chloroform [a) topography and b) phase], xylene [c) topography and d) phase], annealed after spinning from chloroform [e) topography and f) phase] and drop-cast from chloroform [g) topography and h) phase]. Circles denote a dark area in the phase image and the corresponding areas in the topography. Z-range is 10 nm except in drop-cast film where it is 100 nm.<sup>[48]</sup>

(continued)

not have such a high degree of orientation with the substrate. If the crystals were nucleated from the substrate, then changing the interaction between the polymer and substrate by modifying the substrate surface should affect the crystal nucleation. On the other hand, if the crystals were nucleated from the air-film interface, the substrate surface should have minimal effect on the crystal nucleation. In order to determine the crystal location and attempt to control the nucleation, we treated the silicon oxide with self-assembled monolayers (SAMs) to change the surface energy.<sup>[73]</sup>

While the effect of surface treatment on TFT performance has been well established, there have been few conclusive morphology measurements for why it improves mobility. Sirringhaus et al. showed that an HMDS treatment of the silicon oxide substrate improved P3HT mobility over a bare oxide.<sup>[45]</sup> Salleo et al. have shown that treating the silicon oxide

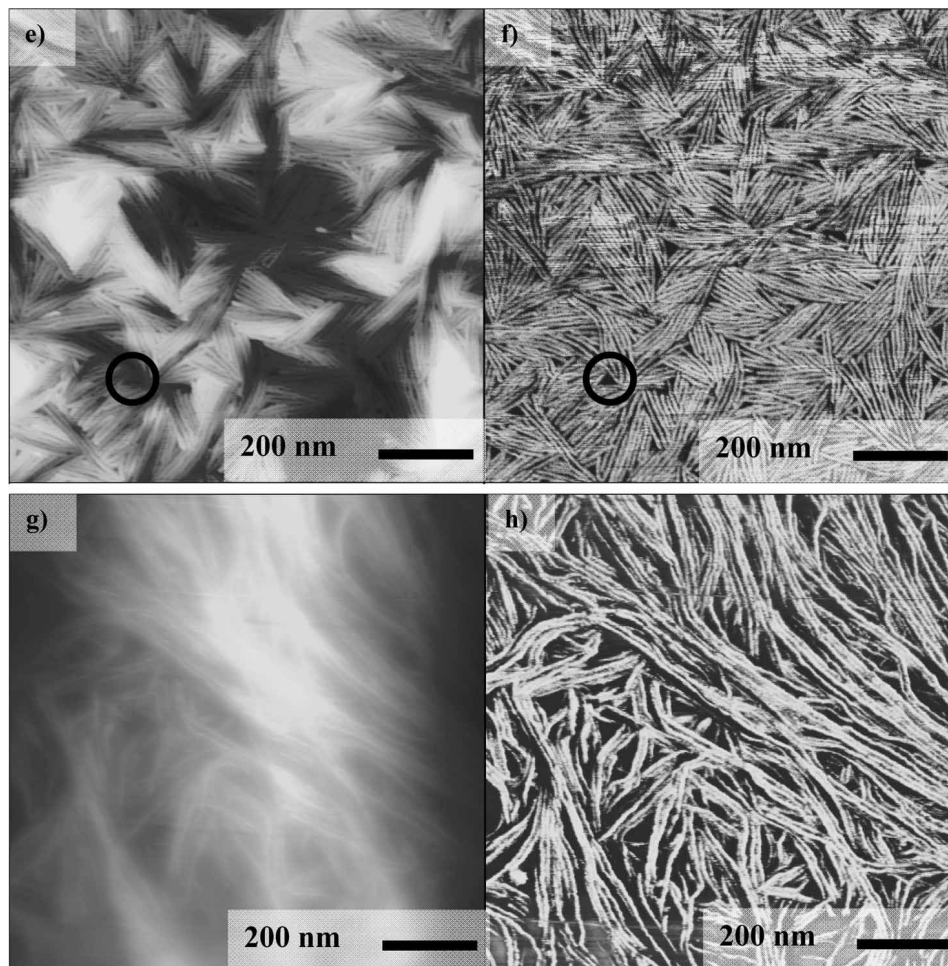
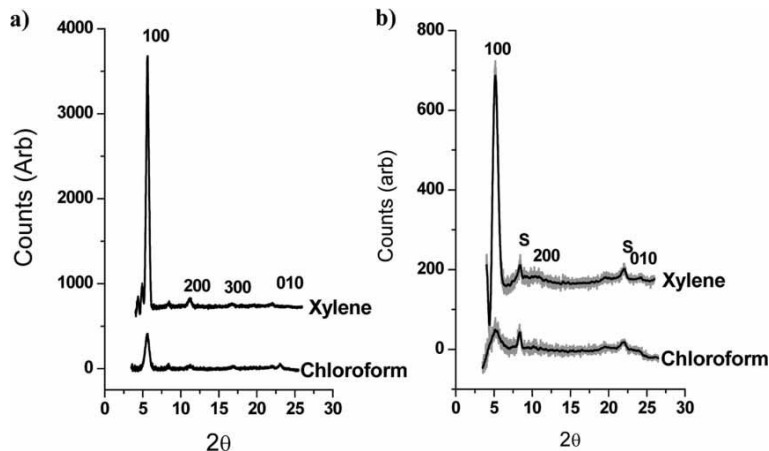


Figure 7. Continued.

with a SAM increases the mobility for both poly(9,9'-dioctylfluorene-co-2,2'-bithiophene)<sup>[74]</sup> and poly[5,58-bis(3-alkyl-2-thienyl)-2,28-bithiophene]<sup>[38]</sup> (PQT). Several other groups have also seen similar effects of surface treatment with P3HT and PQT.<sup>[55,75,76]</sup> Another interesting result is that of Chabinyc et al. where they have shown that a PQT film spin-cast on a SAM-treated silicon oxide can be delaminated from the substrate with polydimethylsiloxane and transferred to another substrate with a variety of surface treatments and TFT electrodes.<sup>[77]</sup> They find that the mobility of the transferred film is independent of the new substrate's surface treatment. Annealing the film on a bare oxide substrate reduces the mobility to that measured for a film cast on a bare oxide. This result suggests that the substrate drives the ordering of at least the first few layers of the film, but provides no information on what the substrate interface is changing about the film.

Similarly to the results of the other processing conditions shown in the previous section, low-MW films are most sensitive to the surface treatment of the substrate. Low-MW films on the more hydrophobic OTS-treated silicon oxide have a mobility 1000 × higher than that cast on HMDS-treated silicon oxide. This increase in mobility



**Figure 8.** Out-of-plane x-ray diffraction. a) low and (b) high-MW films spin-cast from chloroform and xylene are shown. Substrate peaks are marked with s.<sup>[48]</sup>

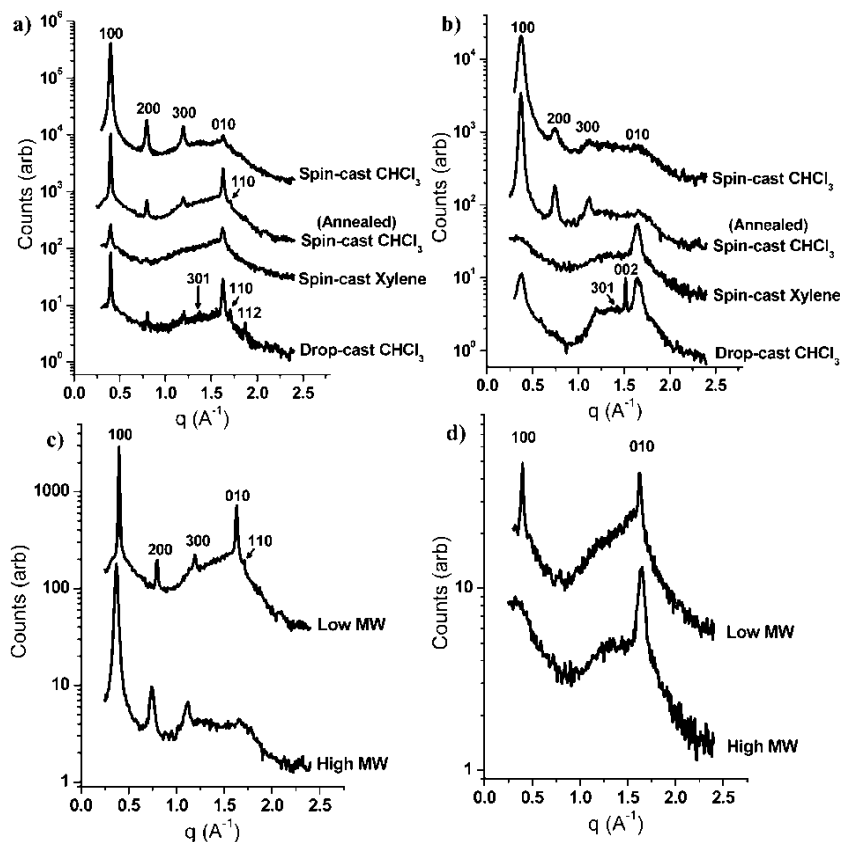


**Figure 9.** In-plane grazing incidence XRD data. a) Low and (b) high-MW films processed by spin-casting from chloroform (before and after anneal), spin-casting from xylene and drop-casting from chloroform are shown. c) compares annealed high and low-MW films spin cast from chloroform and d) compares high and low-MW films spin cast from xylene.<sup>[48]</sup>

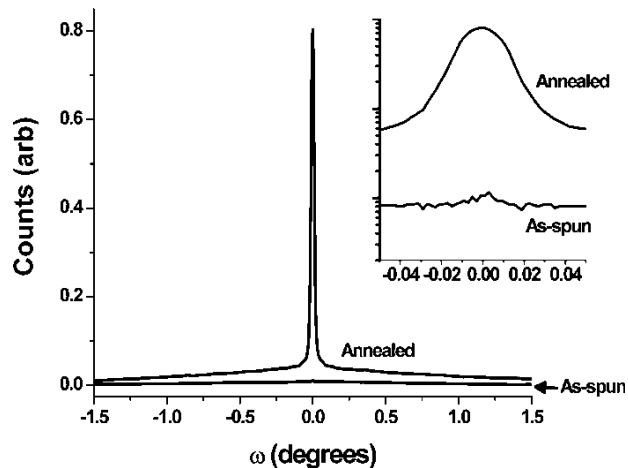


**Figure 10.** Rocking curves of a low-MW film before and after annealing. Inset is zoomed in and plotted on log scale.

is ten times higher than what was achieved for other process modifications for the low-MW films. GIXS measurements of the in-plane diffraction show a large increase in the in-plane  $\pi$ -stacking for the low-MW film on OTS compared to the film on HMDS. This increase agrees with the previous results correlating in-plane  $\pi$ -stacking with mobility. As mentioned in the previous section, the increase in in-plane  $\pi$ -stacking is a result of a net change in crystal orientation and reduces the concentration of insulating grain boundaries in the field of transport, causing more percolation paths for charge to travel through the film. Since the GIXS of low-MW film on OTS showed a large increase in the in-plane  $\pi$ -stacking compared to the one cast on HMDS and the out-of-plane alkyl peaks increased in intensity, our previous results would predict an increase in the concentration of the highly oriented crystals on OTS-treated substrates. Rocking curves confirm this (Fig. 11). The primary difference between low-MW films cast on OTS and those cast on HMDS is the highly oriented crystals. Since the backgrounds of the rocking curves of low-MW films on both substrates are similar and the oriented fraction is different, it seems likely that the highly oriented crystals nucleate from the substrate while the background scattering is in the film bulk and surface. This measurement also shows that the increase in intensity in the out-of-plane (100) Bragg peaks on OTS-treated substrates is entirely due to the oriented crystals. Additional evidence for substrate nucleation comes from AFM images of the substrate and the film surface. The oxidized silicon wafer substrates are flatter than the film surface. The AFM images of the annealed low-MW film cast on HMDS in Fig. 7 shows slope variations of greater than 0.3 degrees. The slope is due to the inclination of the crystals at the top surface and is not due to crystal steps, which would have a step size of 1.5 nm that could be easily resolved with AFM. Since these crystal orientation variations are an order of magnitude greater than the width of the rocking curve peaks for the same films, the crystals cannot be nucleated at the air-film interface.

Rocking curves thus provide a means for measuring crystals at the buried interface with the dielectric where all TFT current travels. The increase in the concentration of oriented

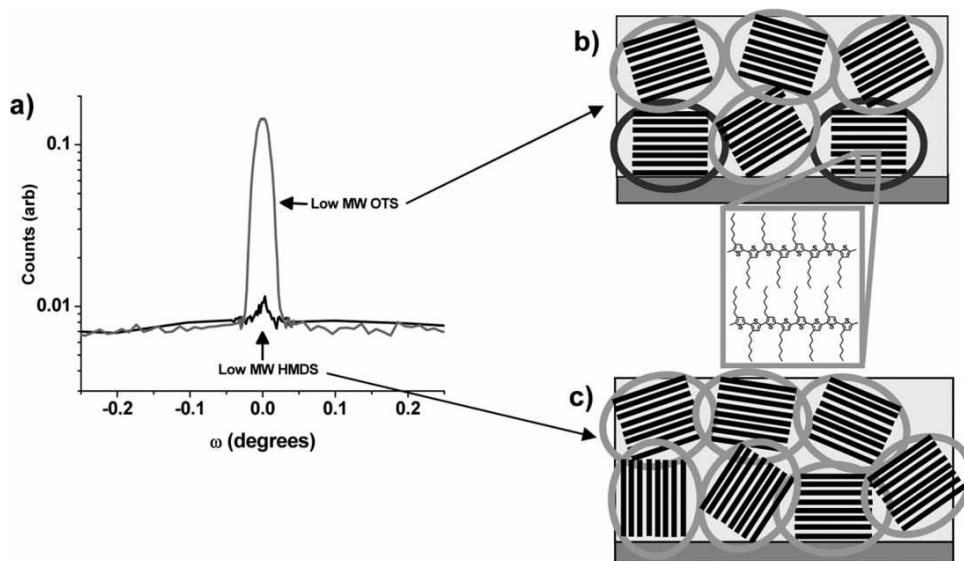


**Figure 11.** Rocking curve measurement on the (100) specular peak showing crystal orientations. (a) Log scale rocking curves comparing low-MW films cast on HMDS and OTS treated substrates. Schematics showing the crystal orientations in (b) low MW on OTS and (c) low-MW on HMDS. Lines correspond to the (100) plane. Black circles denote crystals contributing to the specular diffraction peak and grey curves those that do not.

crystals is expected to increase the number of good grain boundaries in the plane of charge transport by a combination of better overlap between the conducting crystal faces and increased vertical registry of the conjugated planes of neighboring crystals (Fig. 4). The increased vertical registry is a result of crystals nucleating from a flat substrate and is measured by the rocking curve peak width. The peak width of the measured rocking curves corresponds to a lateral coherence length greater than  $10\ \mu\text{m}$ s for the conjugated planes. These results suggest that benefits of in-plane  $\pi$ -stacking for TFT mobility are due to the corresponding increase in electrical connectivity between grains in the plane of charge transport.

## 5. Conclusions

We have presented a series of experiments studying the morphology and charge transport of regioregular P3HT. The MW clearly has a profound effect on both of these properties. As expected, low-MW films have a higher degree of crystallinity than high-MW films. Surprisingly, the less-ordered films have the higher mobility. We have shown that poor connectivity and insulating grain boundaries between misoriented neighboring crystals limit the charge carrier mobility of as-spun low-MW films. Varying the processing by allowing more time for crystallization or by changing the surface treatment causes the crystals to preferentially orient with their insulating side chains normal to the substrate and thus reduces the number of in-plane insulating grain boundaries and increases the charge carrier mobility. The chains of the medium and high-MW films are longer than the domains and minimize the effects of the grain boundaries by bridging neighboring grains.

## References

1. Friend, R.; Gymer, R.; Holmes, A.; et al. "Electroluminescence in conjugated polymers", *Nature* **1999**, *397* (6715), 121–128.
2. Heeger, A. "Semiconducting and metallic polymers: The fourth generation of polymeric materials", *J. Phys. Chem. B.* **2001**, *105* (36), 8475–8491.
3. Hoppe, H.; Sariciftci, N. S. "Organic solar cells: An overview", *J. Mater. Res.* **2004**, *19*, 1924–1944.
4. Coakley, K. M.; McGehee, M. D. "Conjugated polymer photovoltaic cells", *Chem. Mater.* **2004**, *16*, 4533–4542.
5. Katz, H.; Bao, Z. "The physical chemistry of organic field-effect transistors", *J. Phys. Chem. B.* **2000**, *104* (4), 671–678.
6. Dimitrakopoulos, C.; Malenfant, P. "Organic thin film transistors for large area electronics", *Adv. Mater.* **2002**, *14* (2), 99.
7. Chabinyc, M. L.; Salleo, A. "Materials requirements and fabrication of active matrix arrays of organic thin-film transistors for displays", *Chem. Mat.* **2004**, *16* (23), 4509–4521.
8. Horowitz, G. "Organic thin film transistors: From theory to real devices", *J. Mater. Res.* **2004**, *19* (7), 1946–1962.
9. Coakley, K. M.; McGehee, M. D. "Photovoltaic cells made from conjugated polymers infiltrated into mesoporous titania", *Appl. Phys. Lett.* **2003**, *83*, 3380–3382.
10. Schilinsky, P.; Asawapirom, U.; Scherf, U.; et al. "Influence of the molecular weight of poly(3-hexylthiophene) on the performance of bulk heterojunction solar cells", *Chem. Mat.* **2005**, *17* (8), 2175–2180.
11. Chabinyc, M. L.; Lu, J.-P.; Street, R. A.; et al. "Short channel effects in regioregular poly(thiophene) thin film transistors", *J. Appl. Phys.* **2004**, *96* (4), 2063–2070.
12. Basescu, N.; Liu, Z. X.; Moses, D.; et al. "High electrical conductivity in doped polyacetylene", *Nature* **1987**, *327* (6121), 403–405.
13. Chiang, C. K.; Fincher, C. R., Jr.; Park, Y. W.; et al. "Electrical conductivity in doped polyacetylene", *Phys. Rev. Lett.* **1977**, *39* (17), 1098.
14. Naarmann, H.; Theophilou, N. "New process for the production of metal-like, stable polyacetylene", *Synth. Met.* **1987**, *22* (1), 1–8.
15. Genies, E. M.; Boyle, A.; Lapkowski, M.; et al. "Polyaniline: A historical survey", *Synth. Met.* **1990**, *36* (2), 139–182.
16. Chiang, J. C.; Macdiarmid, A. G. Polyaniline: Protonic acid doping of the emeraldine form to the metallic regime. *Synth Met Proc of the Workshop, Synth Met III*, Apr 9–19 1985; Los Alamos, NM, USA, 1985; Vol. 13 (1–3), 193–205.
17. Huang, W. S.; Humphrey, B. D.; Macdiarmid, A. G. "Polyaniline, a novel conducting polymer-morphology and chemistry of its oxidation and reduction in aqueous-electrolytes", *J. Chem. Soc. Faraday Trans. 1* **1986**, *82*, 2385–2400.
18. Mo, Z.; Lee, K. B.; Moon, Y. B.; et al. "X-ray-scattering from polythiophene-crystallinity and crystallographic structure", *Macromolecules* **1985**, *18* (10), 1972–1977.
19. Waltman, R. J.; Bargon, J.; Diaz, A. F. "Electrochemical studies of some conducting polythiophene films", *J. Phys. Chem.* **1983**, *87* (8), 1459–1463.
20. McCullough, R. "The chemistry of conducting polythiophenes", *Adv. Mater.* **1998**, *10* (2), 93–116.
21. Tsumura, A.; Koezuka, H.; Ando, T. "Macromolecular electronic device: Field-effect transistor with a polythiophene thin film", *Appl. Phys. Lett.* **1986**, *49* (18), 1210–1212.
22. Pandey, S.; Takashima, W.; Endo, T.; et al. "Poly(3-butylthiophene): Conjugated polymer with record high of mobility", *Synth. Met.* **2001**, *121* (1–3), 1561–1562.
23. Choulis, S. A.; Nelson, J.; Kim, Y.; et al. "Investigation of transport properties in polymer/fullerene blends using time-of-flight photocurrent measurements", *Appl. Phys. Lett.* **2003**, *83* (18), 3812–3814.



24. Chen, B. J.; Liu, Y. Q.; Lee, C. S.; et al. Carrier transport and high-efficiency electroluminescence properties of copolymer thin films. *Thin Solid Films Asia-Pacific Symposium on Organic Electroluminescent Materials and Devices*, 8–11 June 1999; Hong Kong, 2000; Vol. 363 (1/2), 173–177.
25. Bassler, H. “Injection, transport and recombination of charge carriers in organic light-emitting diodes”, *Polym. Adv. Technol.* **1998**, 9 (7), 402–418.
26. Dicker, G.; De Haas, M. P.; Warman, J. M.; et al. “The disperse charge-carrier kinetics in regioregular poly(3-hexylthiophene)”, *J. Phys. Chem. B.* **2004**, 108 (46), 17818–17824.
27. Lemaire, V.; Da Silva Filho, D. A.; Coropceanu, V.; et al. “Charge transport properties in discotic liquid crystals: A quantum-chemical insight into structure-property relationships”, *J. Am. Chem. S.* **2004**, 126 (10), 3271–3279.
28. Hoofman, R. M.; De Haas, M. P.; Siebbeles, L. D. A.; Warman, J. M. “Highly mobile electrons and holes on isolated chains of the semiconducting polymer poly(phenylene vinylene)”, *Nature* **1998**, 392 (6671), 54–56.
29. Bozano, L.; Carter, S. A.; Scott, J. C.; et al. “Temperature- and field-dependent electron and hole mobilities in polymer light-emitting diodes”, *Appl. Phys. Lett.* **1999**, 74 (8), 1132–1134.
30. Blom, P.; Dejong, M.; Vlegaar, J. “Electron and hole transport in poly(p-phenylene vinylene) devices”, *Appl. Phys. Lett.* **1996**, 68 (23), 3308–3310.
31. Goh, C.; Kline, R. J.; McGehee, M. D.; et al. “Molecular-weight-dependent mobilities in regioregular poly(3-hexylthiophene) diodes”, *Appl. Phys. Lett.* **2005**, 86 (122110).
32. Mozer, A. J.; Sariciftci, N. S. “Negative electric field dependence of charge carrier drift mobility in conjugated, semiconducting polymers”, *Chem. Phys. Lett.* **2004**, 389, 438–442.
33. Tanase, C.; Meijer, E. J.; Blom, P. W. M.; et al. “Unification of the hole transport in polymeric field-effect transistors and light-emitting diodes”, *Phys. Rev. Lett.* **2003**, 91 (21), 216–601.
34. Sirringhaus, H.; Brown, P. J.; Friend, R. H.; et al. “Two-dimensional charge transport in self-organized, high-mobility conjugated polymers”, *Nature* **1999**, 401 (6754), 685–688.
35. Tanase, C.; Blom, P. W. M.; De Leeuw, D. M.; Meijer, E. J. “Charge carrier density dependence of the hole mobility in poly(p-phenylene vinylene)”, *Phys. Status Solidi A (Germany)* **2004**, 201 (6), 1236–1245.
36. Bassler, H. “Charge transport in disordered organic photoconductors. A monte carlo simulation study”, *Phys. Status Solidi B (Germany)* **1993**, 175 (1), 15–56.
37. Vissenberg, M. C. J. M.; Matters, M. “Theory of the field-effect mobility in amorphous organic transistors”, *Phys. Rev. B, Condens. Matter (USA)* **1998**, 57 (20), 12964–12967.
38. Salleo, A.; Chen, T. W.; Volkel, A. R.; et al. “Intrinsic hole mobility and trapping in a regioregular poly(thiophene)”, *Phys. Rev. B.* **2004**, 70 (11), 115–311.
39. Horowitz, G.; Hajlaoui, M.; Hajlaoui, R. “Temperature and gate voltage dependence of hole mobility in polycrystalline oligothiophene thin film transistors”, *J. Appl. Phys.* **2000**, 87 (9), 4456–4463.
40. Horowitz, G. “Organic field-effect transistors”, *Adv. Mater.* **1998**, 10 (5), 365–377.
41. Chesterfield, R. J.; Mckeen, J. C.; Newman, C. R.; et al. “Organic thin film transistors based on n-alkyl perylene diimides: Charge transport kinetics as a function of gate voltage and temperature”, *J. Phys. Chem. B.* **2004**, 108 (50), 19281–19292.
42. Chen, T. A.; Rieke, R. D. “The 1st regioregular head-to-tail poly(3-hexylthiophene-2,5-diyl) and a regiorandom isopolymer-ni vs. pd catalysis of 2(5)-bromo-5(2)-(bromozincio)-3-hexylthiophene polymerization”, *J. Am. Chem. S.* **1992**, 114 (25), 10087–10088.
43. McCullough, R. D.; Lowe, R. D. “Enhanced electrical-conductivity in regioselectively synthesized poly(3-alkylthiophenes)”, *J. Chem. Soc.-Chem. Commun.* **1992**, 1, 70–72.
44. Bao, Z.; Dodabalapur, A.; Lovinger, A. “Soluble and processable regioregular poly(3-hexylthiophene) for thin film field-effect transistor applications with high mobility”, *Appl. Phys. Lett.* **1996**, 69 (26), 4108–4110.
45. Sirringhaus, H.; Tessler, N.; Friend, R. H. “Integrated optoelectronic devices based on conjugated polymers”, *Science* **1998**, 280, 1741.

46. Osterbacka, R.; An, C. P.; Jiang, X. M.; et al. "Two-dimensional electronic excitations in self-assembled conjugated polymer nanocrystals", *Science* **2000**, *287* (5454), 839–842.
47. Winokur, M. J.; Chunwachirasiri, W. "Nanoscale structure-property relationships in conjugated polymers: Implications for present and future device applications", *J. Polym. Sci. B, Polym. Phys. (USA)* **2003**, *41* (21), 2630–2648.
48. Kline, R. J.; McGehee, M. D.; Kadnikova, E. N.; et al. "Dependence of regioregular poly(3-hexylthiophene) film morphology and field-effect mobility on molecular weight", *Macromolecules* **2005**, *38* (8), 3312–3319.
49. Prosa, T.; Winokur, M.; McCullough, R. "Evidence of a novel side chain structure in regioregular poly(3-alkylthiophenes)", *Macromolecules* **1996**, *29* (10), 3654–3656.
50. Prosa, T.; Moulton, J.; Heeger, A.; Winokur, M. "Diffraction line-shape analysis of poly(3-dodecylthiophene): A study of layer disorder through the liquid crystalline polymer transition", *Macromolecules* **1999**, *32* (12), 4000–4009.
51. Toney, M. F.; Russell, T. P.; Logan, J. A.; et al. "Near-surface alignment of polymers in rubbed films", *Nature* **1995**, *374* (6524), 709–711.
52. Factor, B. J.; Russell, T. P.; Toney, M. F. "Surface-induced ordering of an aromatic polyimide", *Phys. Rev. Lett.* **1991**, *66* (9), 1181–1184.
53. Chang, J. F.; Sun, B. Q.; Breiby, D. W.; et al. "Enhanced mobility of poly(3-hexylthiophene) transistors by spin-coating from high-boiling-point solvents", *Chem. Mat.* **2004**, *16* (23), 4772–4776.
54. Sandberg, H.; Frey, G.; Shkunov, M.; et al. "Ultrathin regioregular poly(3-hexyl thiophene) field-effect transistors", *Langmuir* **2002**, *18* (26), 10176–10182.
55. Kim, D. H.; Park, Y. D.; Jang, Y.; et al. "Enhancement of field-effect mobility due to surface-mediated molecular ordering in regioregular polythiophene thin film transistors", *Adv. Mater.* **2005**, *15* (1), 77–82.
56. Yang, H.; Shin, T. J.; Yang, L.; et al. "Effect of mesoscale crystalline structure on the field-effect mobility of regioregular poly(3-hexyl thiophene) in thin-film transistors", *Adv. Funct. Mater.* **2005**, *15* (4), 671–676.
57. Breiby, D. W.; Samuelsen, E. J. "Quantification of preferential orientation in conjugated polymers using x-ray diffraction", *J. Polym. Sci. Pt. B-Polym. Phys.* **2003**, *41* (20), 2375–2393.
58. Aasmundtveit, K. E.; Samuelsen, E. J.; Guldstein, M.; et al. "Structural anisotropy of poly(alkylthiophene) films", *Macromolecules* **2000**, *33* (8), 3120–3127.
59. Knaapila, M.; Stepanyan, R.; Lyons, B. P.; et al. "The influence of the molecular weight on the thermotropic alignment and self-organized structure formation of branched side chain hairy-rod polyfluorene in thin films", *Macromolecules* **2005**, *38* (7), 2744–2753.
60. Knaapila, M.; Kisko, K.; Lyons, B. P.; et al. "Influence of molecular weight on self-organization, uniaxial alignment, and surface morphology of hairy-rodlike polyfluorene in thin films", *J. Phys. Chem. B.* **2004**, *108* (30), 10711–10720.
61. Knaapila, M.; Torkkeli, M.; Jokela, K.; et al. "Diffraction analysis of highly ordered smectic supramolecules of conjugated rodlike polymers", *Journal of Applied Crystallography 12th International Conference on Small-Angle Scattering*, 25–29 Aug. 2002; Venice, Italy, **2003**, *36*, 702–707.
62. Knaapila, M.; Lyons, B. P.; Kisko, K.; et al. "X-ray diffraction studies of multiple orientation in poly(9,9-bis(2-ethylhexyl)fluorene-2,7-diyl) thin films", *J. Phys. Chem. B.* **2003**, *107* (45), 12425–12430.
63. Jung, Y.; Cho, T. Y.; Yoon, D. Y.; Frank, C. W.; Luning, J. "Surface characteristics of polyfluorene films studied by polarization-dependent nexafs spectroscopy", *Macromolecules* **2005**, *38* (3), 867–872.
64. Kim, D. H.; Jang, Y.; Park, Y. D.; Cho, K. "Surface-induced conformational changes in poly(3-hexylthiophene) monolayer films", *Langmuir* **2005**, *21* (8), 3203–3206.
65. Delongchamp, D. M.; Vogel, B. M.; Jung, Y.; et al. "Variations in semiconducting polymer microstructure and hole mobility with spin-coating speed", *Chem. Mater.* **2005**, *17* (23), 5610–5612.

66. Kline, R. J.; McGehee, M. D.; Kadnikova, E. N.; et al. "Controlling the field-effect mobility of regioregular polythiophene by changing the molecular weight", *Adv. Mater.* **2003**, *15* (18), 1519–1522.
67. Street, R. A.; Northrup, J. E.; Salleo, A. "Transport in polycrystalline polymer thin-film transistors", *Phys. Rev. B.* **2005**, *71* (16), 165–202.
68. Beljonne, D.; Cornil, J.; Siringhaus, H.; et al. "Optical signature of delocalized polarons in conjugated polymers", *Adv. Funct. Mater.* **2001**, *11* (3), 229–234.
69. Zen, A.; Pflaum, J.; Hirschmann, S.; et al. "Effect of molecular weight and annealing of poly(3-hexylthiophene)s on the performance of organic field-effect transistors", *Adv. Funct. Mater.* **2004**, *14* (8), 757–764.
70. Lang, P. "Surface induced ordering effects in soft condensed matter systems", *J. Phys., Condens. Matter. (UK)* **2004**, *16* (23), R699–R720.
71. Brown, G.; Chakrabarti, A. "Surface-induced ordering in block copolymer melts", *J. Chem. Phys.* **1994**, *101* (4), 3310–3317.
72. Gutman, L.; Chakraborty, A. K. "Surface-induced ordering for confined random block copolymers", *J. Chem. Phys.* **1994**, *101* (11), 10074–10091.
73. Kline, R. J.; McGehee, M. D.; Toney, M. F. "Highly oriented crystals at the buried interface in polythiophene thin film transistors". Submitted for Publication.
74. Salleo, A.; Chabinyc, M.; Yang, M.; Street, R. "Polymer thin-film transistors with chemically modified dielectric interfaces", *Appl. Phys. Lett.* **2002**, *81* (23), 4383–4385.
75. Veres, J.; Ogier, S.; Lloyd, G.; De Leeuw, D. "Gate insulators in organic field-effect transistors", *Chem. Mat.* **2004**, *16* (23), 4543–4555.
76. Wu, Y.; Liu, P.; Ong, B. S.; et al. "Controlled orientation of liquid-crystalline polythiophene semiconductors for high-performance organic thin-film transistors", *Appl. Phys. Lett.* **2005**, *86* (142102), 1–3.
77. Chabinyc, M. L.; Salleo, A.; Wu, Y. L.; et al. "Lamination method for the study of interfaces in polymeric thin film transistors", *J. Am. Chem. S.* **2004**, *126* (43), 13928–13929.